Available online at www.sciencedirect.com
ScienceDirect
International Journal of Heat and Mass Transfer 51 (2008) 3548–3555
International Journal of HEAT and MASS TRANSFER
www.elsevier.com/locate/ijhmt

Linear correlation of heat transfer and friction in helically-finned tubes using five simple groups of parameters

Gregory J. Zdaniuk [a,1], Rogelio Luck [b,*], Louay M. Chamra [b,2]

[a] *Ramboll Whitbybird Ltd., 60 Newman Street, London W1T 3DA, United Kingdom*
[b] *Department of Mechanical Engineering, Mississippi State University, 210 Carpenter Engineering Building, P.O. Box ME, MS 39762-5925, USA*

Received 7 March 2007; received in revised form 19 October 2007
Available online 4 March 2008

Abstract

A linear regression approach was used to correlate experimentally-determined Colburn *j*-factors and Fanning friction factors for flow of liquid water in helically-finned tubes. Experimental data came from eight enhanced tubes with helix angles between 25° and 48°, number of fin starts between 10 and 45, fin height-to-diameter ratios between 0.0199 and 0.0327, and Reynolds numbers ranging from 12,000 to 60,000. The current study revealed that, in helically-finned tubes, logarithms of both friction and Colburn *j*-factors can be correlated with linear combinations of the same five simple groups of parameters and a constant. The proposed functional relationship was tested with independent experimental data yielding excellent results.

Keywords: Friction; Heat transfer; Helically-finned tube; Symbolic regression

1. Introduction

Industrial use of heat transfer enhancement has become widespread. The goal of heat transfer enhancement is to reduce the size and cost of heat exchanger equipment. Webb [1] gives an excellent overview of different enhancement mechanisms available in commercial tubes.

One contemporary enhancement geometry is the helical fin shown in Fig. 1, which is described by several geometric variables. Fig. 1 also provides a pictorial description of these variables, which include: the fin height (e), the fin pitch (p), the helix angle (α), number of starts (N_s), and included angle (β). The fin height is the distance measured from the internal wall of the tube to the top of the fin. The fin pitch is the distance between the centers of two fins measured in the axial direction. The helix angle is the angle the fin forms with the tube axis. The number of starts refers to how many fins one can count around the circumference of the tube. Finally, the angle at which the sides of the fin meet is called the included angle.

An extensive literature survey of research on helically-finned tubes is given in Zdaniuk [2]. Despite a considerable amount of study, the characteristics of flow inside helically-finned tubes are still not very well understood because the physics governing the flow are very complex and experimental data are limited. The current approach to predicting pressure drop and heat transfer in helically-finned tubes is to use algebraic correlations based on least-squares regression. Regression techniques performed on experimental data require mathematical functional form assumptions, which limit their accuracy and generality. To address these limitations, techniques that can effectively overcome the complexity of the problem without *ad hoc* assumptions are needed. One of these techniques is symbolic regression by means of genetic programming.

Genetic programming (GP) is a method that works with a set of possible operators to obtain optimum functional

* Corresponding author. Tel.: +1 662 325 3261; fax: +1 662 325 7223.
E-mail address: luck@me.msstate.edu (R. Luck).
[1] Tel.: +44 20 7631 5291; fax: +44 20 7323 4645.
[2] Tel.: +1 662 325 3261; fax: +1 662 325 7223.

0017-9310/$ - see front matter © 2007 Elsevier Ltd. All rights reserved.
doi:10.1016/j.ijheatmasstransfer.2007.10.022

Nomenclature

a	correlating parameter vector	*St*	Stanton number
D	tube diameter (m)	*t*	average rib width (m)
e	fin height (m)	**v**	vector of correlation constants
f	Fanning friction factor		
j	Colburn *j*-factor: $j = StPr^{2/3}$	*Greek symbols*	
MSE	mean squared error $\mathrm{MSE} = \frac{\sum(\text{value from experiment} - \text{predicted value})^2}{\text{number of measurements}}$	α	helix angle (°)
		β	included angle (°)
N_s	number of fin starts	*Subscripts*	
Nu	Nusselt number	*f*	refers to the friction coefficient
p	axial fin pitch (m)	*j*	refers to the Colburn *j*-factor
Pr	Prandtl number		
Re	Reynolds number		

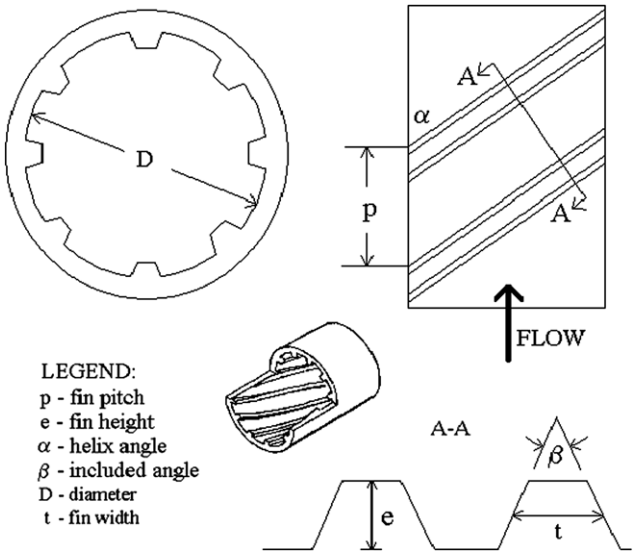

Fig. 1. A helically-finned tube and its geometric variables.

relationships for a given data set [3]. This method should not be confused with the genetic algorithm (GA) which is an optimization technique based on stochastic, evolutionary principles that is used to find global extrema of a given function [4,5]. Sen and Yang [6] described the scope of artificial neural networks[3] and genetic algorithm techniques in thermal science applications including an exhaustive bibliography. Recently, a methodology for obtaining heat transfer correlations by means of symbolic regression was published by Cai et al. [8]. Otherwise, applications of GP in heat transfer are scarce.

2. Experimental data

An experimental program devised to measure turbulent pressure drop and heat transfer in helically-finned tubes was conducted at Mississippi State University. The experimental apparatus and procedure are described in detail in Zdaniuk et al. [9]. Eight enhanced tubes and one plain tube were tested inside a double-pipe counter-flow heat exchanger with hot water flowing on the inside and cold water in the annulus side. The tubes were manufactured for condenser applications. The internal geometric parameters of each tube are delineated in Table 1. The tube material was copper–nickel. The internal fins were 0.48-mm thick at the base and 0.2-mm thick at the tip, yielding an included angle β of 41°. Table 1 lists dimensionless factors e/D, p/e, and p/D. These dimensionless parameters allow a more direct comparison between the tubes and provide more physical insight into the results. Table 1 does not explicitly indicate that the helix angle and the number of starts are dimensionless parameters. However, since these parameters are unitless, they can be treated as such. Therefore, α and N_s can be used as direct parameters in any correlation.

Experimentally determined Fanning friction factors (f) and Colburn j-factors are plotted in Figs. 2 and 3. The uncertainty in the measured friction factor and heat transfer coefficient was calculated at 15% and 10%, respectively. The errors between plain tube results and the Blasius and Dittus-Boelter equations were within the uncertainty limits, thus validating the experimental apparatus.

Zdaniuk et al. [9] used a power law regression-based procedure to correlate the experimental data shown in Figs. 2 and 3 in the following manner:

$$f = 0.128Re^{-0.305}N_s^{0.235}(e/D)^{0.319}\alpha^{0.397} \quad (1)$$

$$j = 0.029Re^{-0.347}N_s^{0.253}(e/D)^{0.0877}\alpha^{0.362} \quad (2)$$

Eqs. (1) and (2) were shown to predict the vast majority of experimental data with an error of less than 10%. The mean squared prediction errors (MSEs) of Eqs. (1) and (2) were $\mathrm{MSE} = 1.070 \times 10^{-6}$ and $\mathrm{MSE} = 6.945 \times 10^{-8}$, respectively. The performance of Eqs. (1) and (2) is illustrated in Figs. 4 and 5, respectively.

[3] Artificial neural networks are another type of artificial intelligence technique [7].

Table 1
Internal geometry of the test tubes

Tube #	Internal structure					Dimensionless factors		
	D (mm)	e (mm)	P (mm)	N_s	α (°)	e/D	p/e	p/D
1	15.64	0.38	10.54	10	25	0.0243	27.729	0.674
2	15.61	0.375	3.51	30	25	0.0240	9.348	0.225
3	15.62	0.38	1.47	30	48	0.0243	3.876	0.0941
4	15.57	0.38	2.33	45	25	0.0244	6.134	0.150
5	15.6	0.31	1.56	45	35	0.0199	5.017	0.100
6	15.57	0.38	1.55	45	35	0.0244	4.085	0.100
7	15.59	0.51	1.55	45	35	0.0327	3.048	0.100
8	15.58	0.38	0.98	45	48	0.0244	2.577	0.0629
9	15.65	Plain						

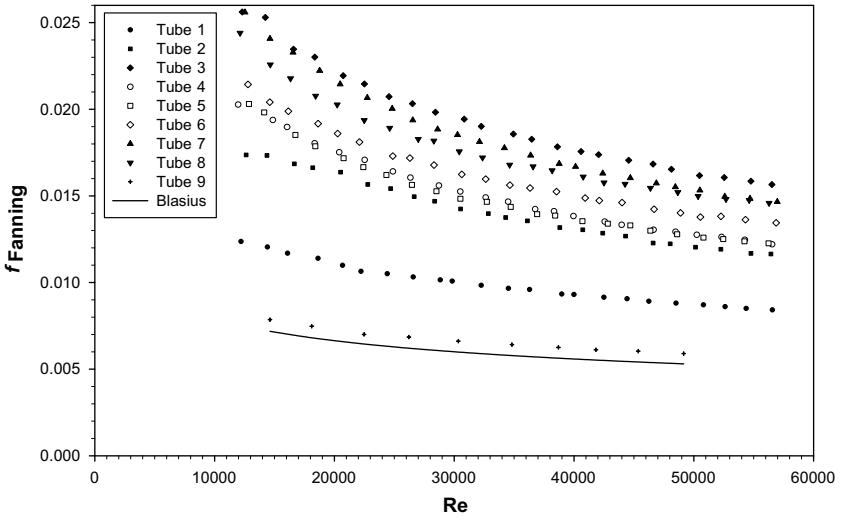

Fig. 2. Measured Fanning friction factors for the eight tube geometries used in the current study, plotted with the Blasius (smooth tube) correlation.

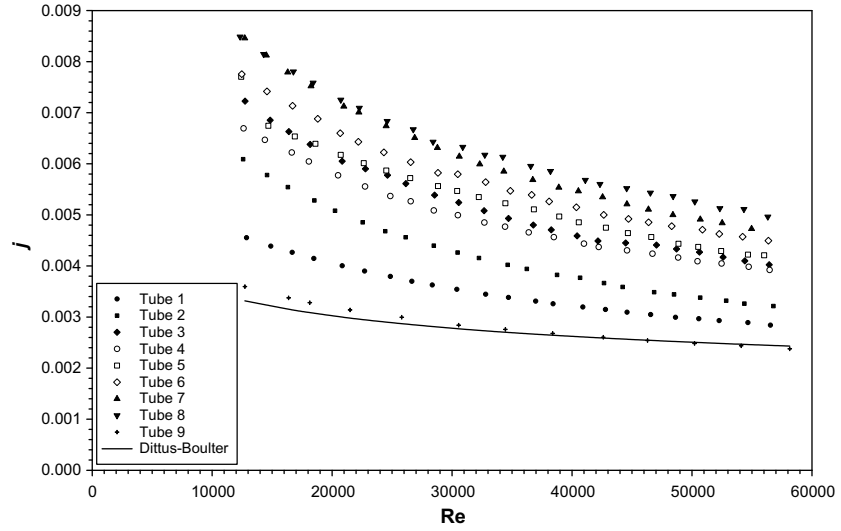

Fig. 3. Measured Colburn j-factors for the eight tube geometries used in the current study, plotted with the Dittus-Boelter (smooth tube) correlation.

Zdaniuk et al. [10] used a feed-forward artificial neural network approach [11] to correlate the experimental data shown in Figs. 2 and 3. Zdaniuk et al. [10] determined that the optimal network architecture to correlate friction or j-factors consisted of 4 log-sigmoid nodes in the input layer and 1 linear node in the output layer. The neural networks performance was superior to the power law correlations, provided enough data were given for training. The 4-1 feed-forward networks trained with 50% of experimental data exhibited outstanding results with mean squared pre-

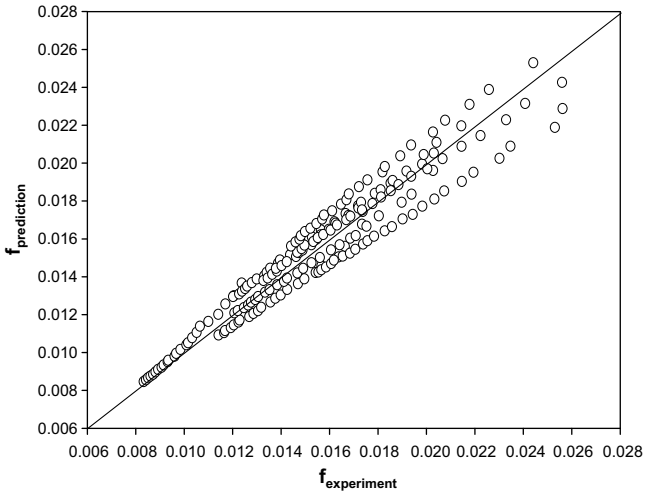

Fig. 4. Scatter plot illustrating the predictive performance of Eq. (1) for Fanning friction factor.

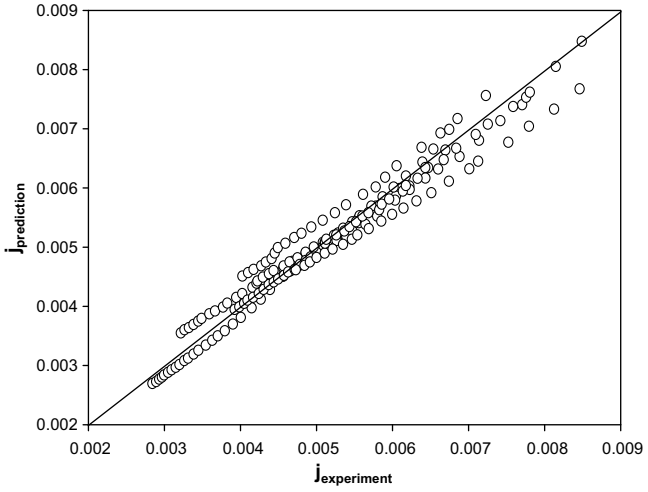

Fig. 5. Scatter plot illustrating the predictive performance of Eq. (2) for Colburn *j*-factor.

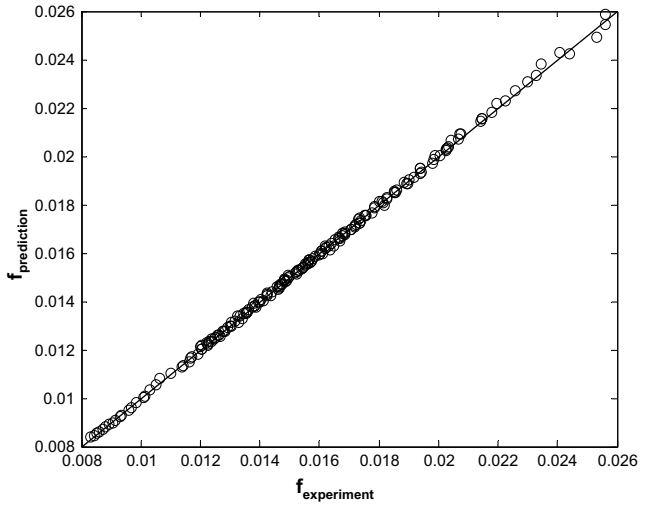

Fig. 6. Scatter plot indicating the performance of the 4-1 feed-forward neural network trained with 50% of friction data.

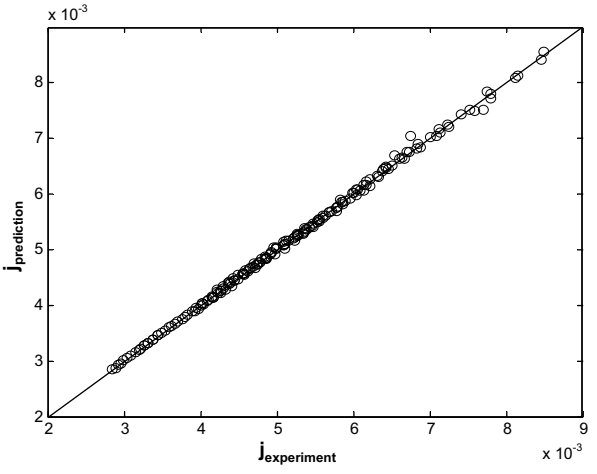

Fig. 7. Scatter plot indicating the performance of the 4-1 feed-forward neural network trained with 50% of *j*-factor data.

diction errors (MSEs) equal to 8.362×10^{-9} for the friction factor network and 1.965×10^{-9} for the Colburn *j*-factor predictions. The performance of these two networks is illustrated in Figs. 6 and 7, respectively.

The artificial neural network (ANN) method is an excellent tool in correlating complex data. The ANN does not know and does not have to know what the physics of the problem are. The ANN completely bypasses simplifying assumptions such as the use of a power-law equation. On the other hand, any unintended and biased errors in the training data set are also picked up by the ANN. As noted by Sen and Yang [6], the trained ANN is therefore not better than the training data, but not worse either. Although the performance of artificial neural networks is superior to algebraic equations, their implementation is not straightforward. For example, the relatively simple 4-1 feed-forward networks mentioned above require 20 constants and linear algebra computations. Simple algebraic correlations such as Eqs. (1) or (2) require much less "computational effort" and can be easily carried out by a handheld calculator. This paper presents simple algebraic correlations that outperform the accuracy of Eqs. (1) and (2).

3. Correlation development

The information presented so far demonstrates that symbolic regression can be a compromise between the complexity of the ANN method and inaccuracy resulting from fitting the data to an assumed functional form (e.g., a power law). The genetic program removes the burden of functional form assumptions and can be controlled to yield uncomplicated equations. The approach taken in this study was to feed the parameters e/D, α, N_s, and $\ln(Re)$ into the genetic program in order to correlate them with $\ln(j)$ and $\ln(f)$. The natural logarithms of Re, f, and j were graphi-

cally identified as more accurate correlating parameters than simply Re, f, and j. The genetic program used for this study was a freely available MATLAB Toolbox developed by Madár et al. [12]. The genetic program identified the following simple groups of parameters:

$$a_1 = e/D \tag{3}$$

$$a_2 = \frac{(e/D)(\alpha)}{N_s} \tag{4}$$

$$a_3 = \alpha N_s \tag{5}$$

$$a_4 = \frac{(e/D)}{N_s} \tag{6}$$

$$a_5 = \ln(Re) \tag{7}$$

An attempt at assigning a physical meaning to the above parameters follows. a_1 is the dimensionless fin height. The a_2 term is of a form proportional to the tube severity factor. Φ defined as e^2/pD [13], which indicates the "intensity" of tube augmentation. Due to the complexities of flow in helically-finned tubes [2], the role of parameters a_3 and a_4 is difficult to identify. Nevertheless, the combination of the two would seem to determine the blockage of flow near the wall and the consequent development of skimming flow. For example, the higher α or N_s the higher the probability that the flow will stall or separate near the wall due to form or shear drag. On the other hand, the higher the e/D, the more likely the flow is to follow the inter-fin space. Finally, parameter a_5 accounts for the Reynolds number dependence.

Rather than relying on the genetic program to correlate the parameters a_1 through a_5, the idea was to test their linear combination such that

$$\ln(f) = v_{f,1}(e/D) + v_{f,2}\frac{(e/D)(\alpha)}{N_s} + v_{f,3}(\alpha N_s) + v_{f,4}\frac{(e/D)}{N_s} + v_{f,5}\ln(Re) + v_{f,6} \tag{8}$$

and

$$\ln(j) = v_{j,1}(e/D) + v_{j,2}\frac{(e/D)(\alpha)}{N_s} + v_{j,3}(\alpha N_s) + v_{j,4}\frac{(e/D)}{N_s} + v_{j,5}\ln(Re) + v_{j,6} \tag{9}$$

where $v_{f,1}$ through $v_{f,6}$ and $v_{j,1}$ through $v_{j,6}$ are constants to be determined. Both f and j were assumed to depend on the same parameters following the theory of heat-momentum analogy [14]. Eqs. (8) and (9) can be rewritten using matrix algebra:

$$\ln(f) = \mathbf{v}_f \cdot \mathbf{a} \tag{10}$$

$$\ln(j) = \mathbf{v}_j \cdot \mathbf{a} \tag{11}$$

where $\mathbf{v}_f$ and $\mathbf{v}_j$ are vectors of constants and $\mathbf{a}$ is the correlating parameter vector

$$\mathbf{a} = \begin{bmatrix} a_1 \\ a_2 \\ a_3 \\ a_4 \\ a_5 \\ 1 \end{bmatrix} \tag{12}$$

As can be seen, the form of Eqs. (10) and (11) is very simple. In order to find constants $\mathbf{v}_f$ and $\mathbf{v}_j$, Eqs. (10) and (11) are written for each data point and a weighted least squares regression is performed [15]. Note that Eqs. (10) and (11) are nonlinear in f or j but linear in $\ln(f)$ or $\ln(j)$. Using a first-order Taylor series approximation one obtains $\ln(f) - \ln(f_o) = (1/f_o)(f - f_o)$ implying that an error in $\ln(f)$ is, to a first-order approximation, proportional to an error in f, where the proportionality multiplier factor is $(1/f_o)$. The same is done for the expansion of $\ln(j)$. As a result, a weighted least squares using the reciprocals of f and j as the weights is used in the linear regression for Eqs. (10) and (11). For the experimental data of the current study, the constants $\mathbf{v}_f$ and $\mathbf{v}_j$ were found to be

$$\mathbf{v}_f = [\,7.893 \quad 17.799 \quad -5.283\times10^{-5} \quad -692.383 \quad -0.330 \quad -1.027\,] \tag{13}$$

and

$$\mathbf{v}_j = [\,12.666 \quad -1.220 \quad 2.598\times10^{-4} \quad -38.656 \quad -0.374 \quad -2.004\,] \tag{14}$$

so that

$$\ln(f) = 17.893(e/D) + 17.799\frac{(e/D)(\alpha)}{N_s} - 5.283\times10^{-5}\alpha N_s - 692.383\frac{(e/D)}{N_s} - 0.33\ln(Re) - 1.027 \tag{15}$$

$$\ln(j) = 12.666(e/D) - 1.220\frac{(e/D)(\alpha)}{N_s} + 2.598\times10^{-4}\alpha N_s - 38.656\frac{(e/D)}{N_s} - 0.374\ln(Re) - 2.004 \tag{16}$$

Eq. (15) predicts experimental friction factors with a MSE of 7.564×10^{-8} (versus 8.362×10^{-9} for the ANN and 1.070×10^{-6} for Eq. (1)) and the comparison of predicted and experimentally-determined friction factors is illustrated in Fig. 8. Similarly, Eq. (16) predicts experimental Colburn j-factors with a MSE of 1.640×10^{-8} (versus

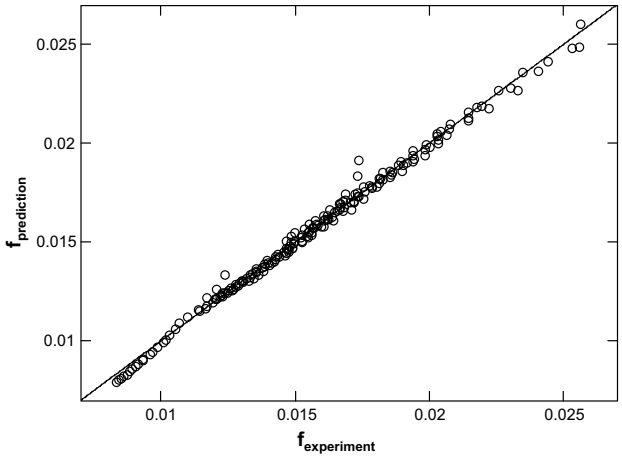

Fig. 8. Scatter plot indicating the predictive performance of Eq. (15).

1.965×10^{-9} for the ANN and 6.945×10^{-8} for Eq. (2)) and the comparison of predicted and experimentally-determined j-factors is shown in Fig. 9. Figs. 8 and 9 demonstrate that Eqs. (15) and (16) predict experimental data very well. The highest errors were associated with tube 1 where a different Reynolds number dependence can be noticed for both friction and j-factors. This inconsistency could be linked to the fact that tube 1 had only 10 starts and 25° helix angle and demonstrated more smooth-tube like behavior compared to the remaining tubes (see Figs. 2 and 3). Nonetheless, Figs. 8 and 9, as well as the mean squared errors demonstrate that Eqs. (15) and (16) with a linear combination of five terms obtained from a set of four independent variables, predict experimental data much better than Eqs. (1) and (2) with a power law applied to the same four independent variables. Neither prediction is nearly as good as that of the artificial neural networks which contained 20 degrees of freedom. Of course, one would expect an improvement in performance as the number of coefficients to be determined is increased from four to five and then to 20. For most practical purposes, the simplicity of Eqs. (15) and (16) is worth the minor loss of accuracy relative to the artificial neural network approach. Finally, it is important to mention that Eqs. (15) and (16) fail to predict hydraulic and thermal performance of smooth tubes.

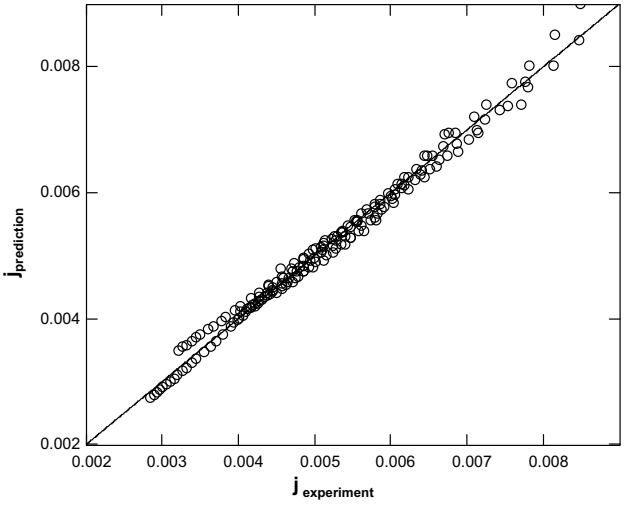

Fig. 9. Scatter plot indicating the predictive performance of Eq. (16).

4. Evaluation of the proposed functional form with independent experimental data

Webb et al. [16] used a double-pipe counter-flow heat exchanger set up with liquid water on the inside and boiling R-12 on the annulus side to measure Fanning friction factors and Colburn j-factors of eight helically-finned tubes at Reynolds numbers between 20,000 and 80,000. Table 2 provides the internal geometry of the helically-finned tubes tested by Webb et al. [16]. Table 2 tubes are numbered W1 through W8 in order to distinguish them from the tubes used in the current study.

Zdaniuk et al. [9,10] evaluated the performance of Eqs. (1) and (2) and the artificial neural networks with experimental data of Webb et al. [16] and concluded that there is a bias error between the experimental data of the current study and that of Webb et al. [16]. Therefore, the objective of this section is to simply test the functional form of Eqs. (8) and (9) rather than to predict the data of Webb et al. [16] with Eqs. (15) and (16). With this in mind, the experimental data of Webb et al. [16] was used to perform a least squares regression in order to determine new constants $\mathbf{v}_f$ and $\mathbf{v}_j$:

$$\mathbf{v}_f = [13.260 \quad 8.077 \quad 9.594 \times 10^{-5} \quad -400.516 \quad -0.287 \quad -1.802] \tag{17}$$

and

$$\mathbf{v}_j = [-1.192 \times 10^{-2} \quad 7.282 \quad -1.515 \times 10^{-4} \quad -560.4 \quad -0.1752 \quad -2.629] \tag{18}$$

The equations that correlate the data of Webb et al. [16] are then

$$\ln(f) = 13.26(e/D) + 8.077\frac{(e/D)(\alpha)}{N_s} + 9.594 \times 10^{-5}\alpha N_s - 400.516\frac{(e/D)}{N_s} - 0.287\ln(Re) - 1.802 \tag{19}$$

$$\ln(j) = -1.192 \times 10^{-2}(e/D) + 7.282\frac{(e/D)(\alpha)}{N_s} - 1.515 \times 10^{-4}\alpha N_s - 560.4\frac{(e/D)}{N_s} - 0.1752\ln(Re) - 2.629 \tag{20}$$

Eq. (19) predicts Webb et al. [16] friction factors with a MSE of 8.702×10^{-8}. This performance is shown graphically in Fig. 10. Similarly, Eq. (20) predicts Webb et al.

Table 2
Tubes tested by Webb et al. [16]

Tube #	I.D. (mm)	E (mm)	p (mm)	t (mm)	N_s	α	e/D	p/e	p/D
W1	15.54	plain							
W2	15.54	0.327	1.08	0.265	45	45°	0.0210	2.81	0.0591
W3	15.54	0.398	1.63	0.28	30	45°	0.0256	3.50	0.0896
W4	15.54	0.43	4.88	0.325	10	45°	0.0277	9.88	0.273
W5	15.54	0.466	1.74	0.275	40	35°	0.0300	3.31	0.0993
W6	15.54	0.493	2.79	0.28	25	35°	0.0317	5.02	0.159
W7	15.54	0.532	4.19	0.28	25	25°	0.0342	7.05	0.241
W8	15.54	0.554	5.82	0.28	18	25°	0.0356	9.77	0.348

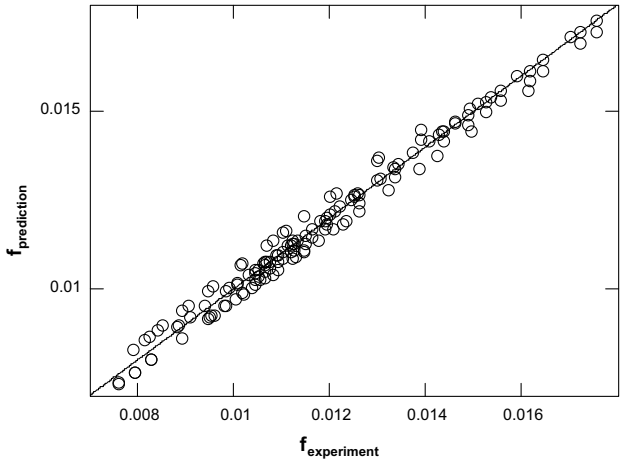

Fig. 10. Scatter plot indicating the performance of Eq. (19) for friction factors of Webb et al. [16].

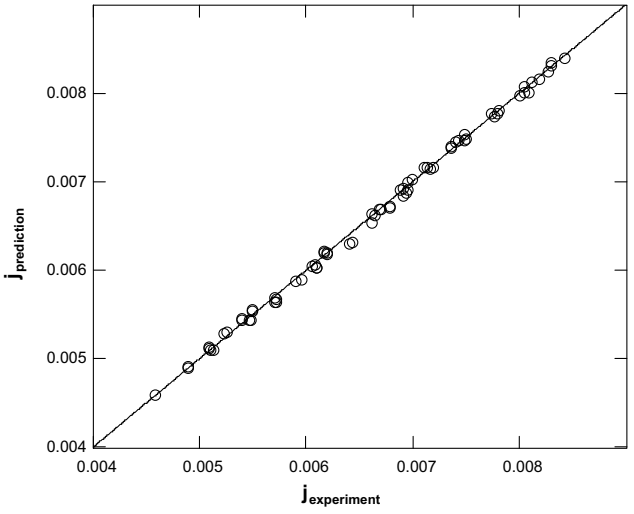

Fig. 11. Scatter plot indicating the performance of Eq. (20) for j-factors of Webb et al. [16].

[16] j-factors with a MSE of 1.930×10^{-9} and its performance shown graphically in Fig. 11. Figs. 10 and 11, as well as the mean squared errors demonstrate that Eqs. (19) and (20) correlate the data of Webb et al. [16] very well, but again, do not perform well for prediction of smooth tube performance.

5. Conclusions

The principal finding of the current investigation is the fact that in helically-finned tubes both Fanning friction factors and Colburn j-factors can be correlated with exponentials of linear combinations of the same five simple groups of parameters and a constant. The performance of the proposed correlations is much better than that of the power-law correlations and only slightly worse than that of the artificial neural networks. The functional form proposed in Eqs. (8) or (9) works very well for the data of the current study and Webb et al. [16].

References

[1] R.L. Webb, Performance, cost effectiveness, and water-side fouling considerations of enhanced tube heat exchangers for boiling service with tube-side water flow, Heat Transfer Eng. 3 (1982) 84–98.
[2] G.J. Zdaniuk, Heat transfer and friction in helically-finned tubes using artificial neural networks, PhD dissertation, Mississippi State University, Mississippi State, MS, 2006.
[3] J.R. Koza, Genetic Programming Paradigm, On the Programming of Computers by Means of Natural Selection, The MIT Press, Cambridge, MA, 1992.
[4] J.H. Holland, Adaptation in Natural and Artificial Systems, University of Michigan Press, Ann Arbor, MI, 1975.
[5] D.E. Goldberg, Genetic Algorithms in Search, Optimization and Machine Learning, Addison-Wesley, Reading, MA, 1989.
[6] M. Sen, K.T. Yang, Applications of artificial neural networks and genetic algorithms in thermal engineering, in: F. Kreith (Ed.), The CRC Handbook of Thermal Engineering, CRC Press, Boca Raton, FL, 2000, pp. 620–661.
[7] K. Mehrotra, C.M. Mohan, S. Ranka, Elements of Artificial Neural Networks (Complex Adaptive Systems), The MIT Press, Cambridge, MA, 1996.
[8] W. Cai, A. Pachego-Vega, M. Sen, K.T. Yang, Heat transfer correlations by symbolic regression, Int. J. Heat Mass Transfer 49 (2006) 4352–4359.
[9] G.J. Zdaniuk, L.M. Chamra, P.J. Mago, Experimental determination of heat transfer and friction in helically-finned tubes, Exp. Thermal Fluid Sci., in press, doi:10.1016/j.expthermflusci.2007.09.006.
[10] G.J. Zdaniuk, L.M. Chamra, D.K. Walters, Correlating heat transfer and friction in helically-finned tubes using artificial neural networks, Int. J. Heat Mass Transfer 50 (2007) 4713–4723.
[11] M. Hagan, H. Demuth, M. Beale, Neural Network Design, PWS Publishing, Boston, MA, 1996.
[12] J. Madár, J. Abonyi, F. Szeifert, Genetic programming for the identification of nonlinear input-output models, Ind. Eng. Chem. Res. 44 (2005) 3178–3186.
[13] R.K. Gupta, M.R. Rao, Heat transfer and friction characteristics of newtonian and power-law type of non-newtonian fluids in smooth

and spirally corrugated tubes, in: Proceedings of the 18th National Heat Transfer Conference in San Diego, CA, American Society of Mechanical Engineers, August 6–8, 1979, pp. 103–113.

[14] D.F. Dipprey, R.H. Sabersky, Heat and momentum transfer in smooth and rough tubes at various Prandtl numbers, Int. J. Heat Mass Transfer 6 (1963) 329–353.

[15] G. Strang, Introduction to Linear Algebra, second ed., Wellesley-Cambridge Press, Wellesley, MA, 1993.

[16] R.L. Webb, R. Narayanamurthy, P. Thors, Heat transfer and friction characteristics of internal helical-rib roughness, Trans. ASME: J. Heat Transfer 122 (2000) 134–142.